



Hydrogen bonding in the crystal structure of molnupiravir Form I, C₁₃H₁₉N₃O₇

Tawnee M. Ens,¹ James A. Kaduk ,^{1,2} Megan M. Rost,³ Anja Dosen ,^{3,a)} and Thomas N. Blanton ³

¹North Central College, 131 S. Loomis St., Naperville, IL 60540, USA

²Illinois Institute of Technology, 3101 S. Dearborn St., Chicago, IL 60616, USA

³ICDD, 12 Campus Blvd., Newtown Square, PA 19073-3273, USA

(Received 5 July 2024; accepted 6 November 2024)

Molnupiravir Form I crystallizes in space group *C*2 (#5) with $a = 6.48110(17)$, $b = 8.71848(19)$, $c = 27.0607(19)$ Å, $\beta = 91.920(4)^\circ$, $V = 1528.22(12)$ Å³, and $Z = 4$ at 295 K. The crystal structure consists of supramolecular double layers of molecules parallel to the *ab*-plane. The layer centers consist of hydrogen-bonded rings forming a 2D network and the outer surfaces of isopropyl groups, with van der Waals interactions between the layers. Each O atom acts as an acceptor in at least one hydrogen bond. A strong O–H...O hydrogen bond forms between the hydroxyl group of the oxolane ring and the carbonyl group of the oxopyrimidine ring. The other oxolane hydroxyl group forms bifurcated intra- and intermolecular hydrogen bonds. The hydroxylamino group forms an intramolecular O–H...N hydrogen bond with an N atom of the oxopyrimidine ring. The amino group forms an intermolecular N–H...N hydrogen bond to the same N atom of the ring. The powder pattern has been submitted to ICDD for inclusion in the Powder Diffraction File™ (PDF®).

© The Author(s), 2025. Published by Cambridge University Press on behalf of International Centre for Diffraction Data. This is an Open Access article, distributed under the terms of the Creative Commons Attribution licence (<http://creativecommons.org/licenses/by/4.0/>), which permits unrestricted re-use, distribution and reproduction, provided the original article is properly cited.

[doi:10.1017/S0885715624000599]

Key words: molnupiravir, Lagevrio™, crystal structure, Rietveld refinement, density functional theory

I. INTRODUCTION

Molnupiravir (Lagevrio) is an FDA-approved antiviral for the treatment of mild to moderate COVID-19, targeting high-risk individuals (Cavazzoni, 2023). It disrupts the RNA-dependent RNA Polymerase (RdRp) enzyme, hindering the coronavirus and RNA replication (Painter et al., 2021; Singh et al., 2021). This drug inactivates viral replication by accruing deleterious mutations in the RdRp enzyme, rendering the virus ineffective via mutagenesis (Caraco et al., 2022). The systematic name (CAS Registry Number 2349386-89-4) is [(2*R*,3*S*,4*R*,5*R*)-3,4-dihydroxy-5-[4-(hydroxyamino)-2-oxopyrimidin-1-yl]oxolan-2-yl]methyl 2-methylpropanoate.

The patent history of molnupiravir has been reviewed by Imran et al. (2021). A powder pattern for molnupiravir crystal Form A has been reported in Chinese Patent CN112778387 (Xuchun et al., 2021). Powder patterns of Forms I and II are reported in International Patent Application WO 2022/047229 A1 (Bothe et al., 2022). A picture of the molecule in the crystal structure is provided, but atom coordinates are not reported. During the course of this work, the crystal structure was reported by Bade et al. (2023) and Han et al. (2024).

This work is part of a project (Kaduk et al., 2014) to determine commercial pharmaceutical crystal structures and add

high-quality powder diffraction data to the Powder Diffraction File (Kabekkodu et al., 2024).

II. EXPERIMENTAL AND ANALYSIS

Molnupiravir was a white powder purchased from TargetMol (Batch #226219) and analyzed at 295 K at 11-BM (Antao et al., 2008; Lee et al., 2008; Wang et al., 2008) at APS using a wavelength of 0.459744(2) Å. The pattern was indexed and the crystal structure was solved independently using Monte Carlo simulated annealing techniques as implemented in FOX (Favre-Nicolin and Černý, 2002), using $(\sin\theta/\lambda)_{\max} = 0.28$ Å⁻¹. Rietveld refinement (Figure 1) was carried out using GSAS-II (Toby and Von Dreele, 2013). The *y*-coordinate of O1 was fixed to define the origin. All non-H bond distances and angles were restrained according to a Mercury/Mogul Geometry Check (Bruno et al., 2004; Sykes et al., 2011). The oxopyrimidine ring was restrained to be planar. Hydrogen atoms were included in calculated positions and recalculated during the refinement using Materials Studio (Dassault Systèmes, 2023). U_{iso} of the carbon, nitrogen, and oxygen atoms were grouped by chemical similarity, while the U_{iso} for H atoms were fixed at 1.3× the U_{iso} of the carbon, nitrogen, and oxygen atoms they are attached to. The final refinement yielded $R_{\text{wp}} = 0.1231$ and $\text{GOF} = 1.76$. The largest features in the normalized error plot are in the shapes of the 001 peaks; the data did not support refining a

^{a)}Author to whom correspondence should be addressed. Electronic mail: dosen@icdd.com



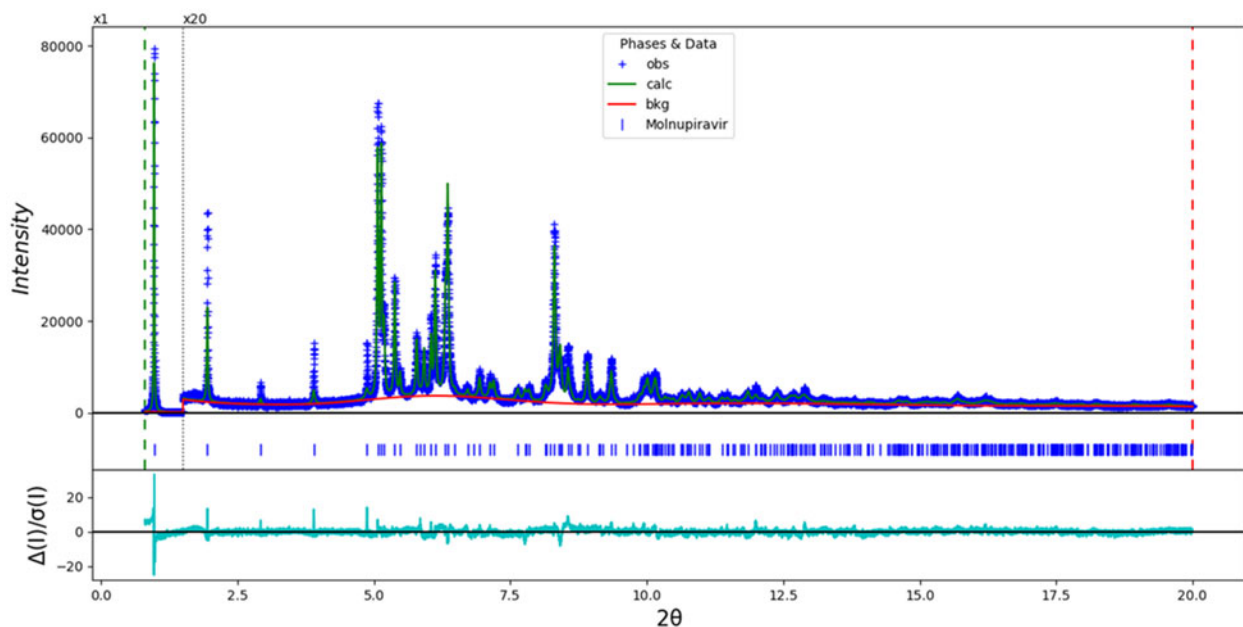


Figure 1. The Rietveld plot for molnupiravir Form I shows observed data (blue crosses) and the calculated pattern (green line). The cyan curve represents the normalized error, and the red line indicates the background. The vertical scale is multiplied by 20× for $2\theta > 1.5^\circ$.

more complex profile function, hence the relatively high residuals. The largest peak (0.31 \AA from O7) and hole (1.91 \AA from N10) in the difference Fourier map were $0.23(6)$ and $-0.21(6) e\text{\AA}^{-3}$, respectively. The crystal structure of molnupiravir was optimized (fixed unit cell) with density functional theory techniques using VASP 6.0 (Kresse and Furthmüller, 1996) through the MedeA graphical interface (Materials Design, 2023). Single-point density functional theory calculations (fixed experimental cell) and population analysis were carried out using CRYSTAL23 (Erba et al., 2023) using base H, C, N, and O sets defined by Gatti et al. (1994).

III. RESULTS AND DISCUSSION

The root-mean-square Cartesian displacement of the non-H atoms in the Rietveld-refined and VASP-optimized molecules is 0.126 \AA , within the normal range for correct structures (van de Streek and Neumann, 2014). The

asymmetric unit with the atom numbering is presented in Figure 2. The side chain's displacement parameters are larger than the ring systems, suggesting possible disorder, but no disorder was modeled as an ordered structure is needed for DFT calculations.

Most bond distances, bond angles, and torsion angles fall within the normal range indicated by a Mercury/Mogul Geometry check (Macrae et al., 2020). Only the N10–C21–N9 114.2° angle (average = $119.7(18)$, Z-score = 3.3) and torsion angles involving the C14–N8 bond rotation are flagged as unusual. The N10–C21–N9 angle reflects the orientation of the hydroxylamino group and the pyrimidine ring. The torsion angles lie on the tails of broad bimodal distributions of similar torsion angles and reflect the orientation of the oxolane ring and the side chain. The ring and side chain participate in numerous hydrogen bonds, indicating that solid-state interactions are important in determining the observed conformation.

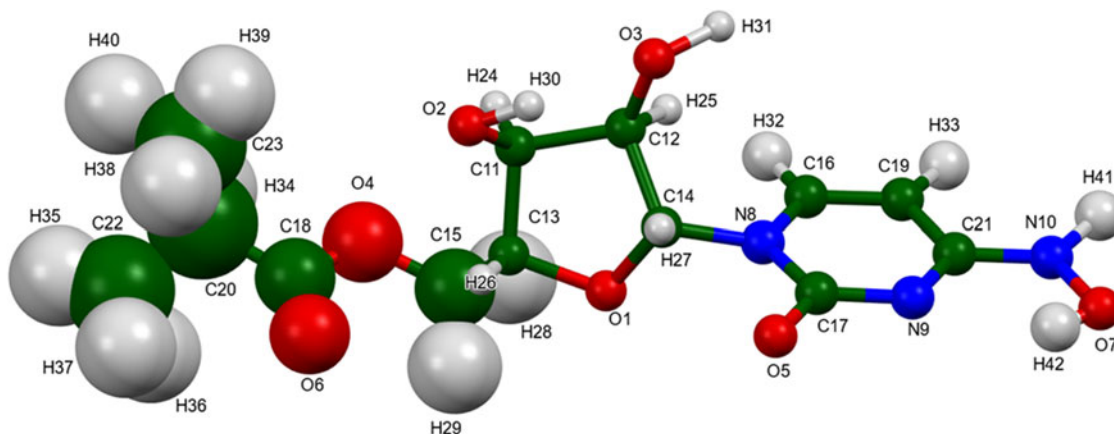


Figure 2. The asymmetric unit of molnupiravir Form I is shown with atom numbering. Atoms are depicted as 50% probability spheroids. Image generated with Mercury (Macrae et al., 2020).

TABLE I. Hydrogen bonds (CRYSTAL23) in molnupiravir Form A.

| H-Bond | D–H (Å) | H...A (Å) | D...A (Å) | D–H...A (°) | Mulliken overlap (<i>e</i>) | E (kcal mol ⁻¹) |
|--------------|---------|--------------------|-----------|-------------|-------------------------------|-----------------------------|
| O3–H31...O5 | 0.997 | 1.671 | 2.661 | 171.8 | 0.058 | 13.2 |
| O2–H30...O3 | 0.983 | 2.142 ^a | 2.625 | 108.5 | 0.023 | 8.3 |
| O2–H30...O1 | 0.983 | 2.528 | 3.404 | 148.3 | 0.015 | 6.7 |
| O7–H42...N9 | 1.000 | 1.796 ^a | 2.515 | 125.8 | 0.053 | |
| N10–H41...N9 | 1.031 | 2.059 | 3.085 | 173.2 | 0.046 | |
| C19–H33...O7 | 1.085 | 2.110 | 3.085 | 148.1 | 0.015 | |
| C16–H32...O2 | 1.087 | 2.757 | 3.750 | 151.6 | 0.014 | |
| C11–H24...O6 | 1.103 | 2.700 | 3.722 | 153.8 | 0.012 | |
| C23–H39...O6 | 1.098 | 2.589 | 3.579 | 149.5 | 0.013 | |
| C23–H38...O4 | 1.099 | 2.460 | 3.559 | 178.8 | 0.015 | |

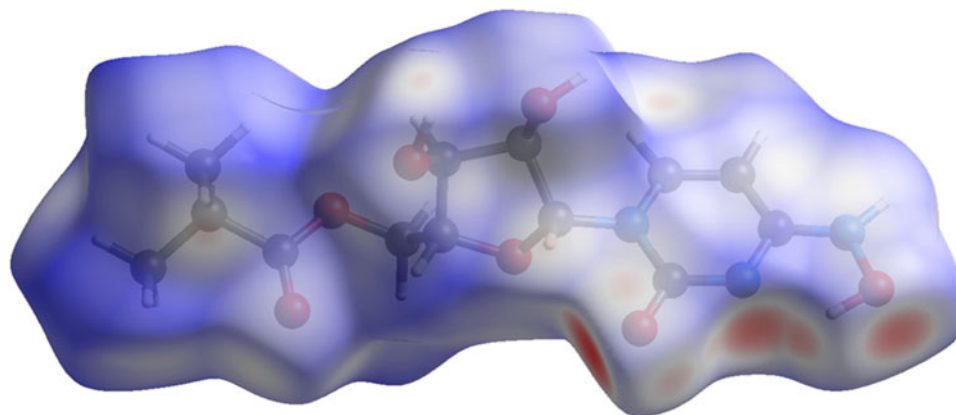
^aIntramolecular.

Figure 3. The Hirshfeld surface of molnupiravir Form I shows intermolecular contacts: blue for longer than van der Waals radii, red for shorter, and white for equal. Image generated with CrystalExplorer (Spackman et al., 2021).

Quantum chemical geometry optimization of the isolated molecule (DFT/B3LYP/6-31G*/water) using Spartan '24 (Wavefunction, 2023) indicated that the solid-state conformation is 7.4 kcal mol⁻¹ higher in energy than a local minimum, which has a different orientation of the oxopyrimidine ring. The global minimum-energy conformation (4.1 kcal mol⁻¹ lower in energy) is much more compact, with the isopropyl group close to the oxopyrazine ring.

The crystal structure consists of supramolecular double layers of molnupiravir molecules parallel to the *ab*-plane. The layers consist of hydrogen-bonded rings, which form a two-dimensional network, while the outer surfaces consist of isopropyl groups, with van der Waals interactions between the layers. The oxopyrimidine ring planes stack parallel along the *a*-axis. The shortest distance between the ring centroids is 5.44 Å. Analysis of the contributions to the total crystal energy of the structure using the Forcite module of Materials Studio (Dassault Systèmes, 2023) suggests that angle and torsion distortion terms contribute significantly to the intramolecular deformation energy while electrostatic repulsions dominate the intermolecular energy.

Hydrogen bonds are prominent in the crystal structure (Table I). Each O atom acts as an acceptor in at least one hydrogen bond. There is a strong O–H...O hydrogen bond between the hydroxyl group O3 and the carbonyl group O5 of the oxopyrimidine ring. Hydroxyl group O2 forms bifurcated hydrogen bonds, one intra- and the other intermolecular. The energies of the O–H...O hydrogen bonds were calculated using the correlation of Rammohan and Kaduk (2018). The

hydroxyl group O7 forms an intramolecular O–H...N hydrogen bond to N9. The amino group N10 forms an intermolecular N–H...N hydrogen bond to N9. These classical hydrogen bonds result in a two-dimensional network parallel to the *ab*-plane. Additionally, there are C–H...O hydrogen bonds from ring and methyl carbon atoms. The methyl group C23 forms hydrogen bonds to the carboxyl group of side chains in adjacent molecules, so the sidechain–sidechain interactions are more complex than van der Waals.

The volume enclosed by the Hirshfeld surface of molnupiravir (Figure 3; Hirshfeld, 1977; Spackman et al., 2021) is 376.99 Å³, 98.67% of the unit cell volume suggesting fairly typical packing density. The only significant close contacts (red in Figure 3) involve the hydrogen bonds. The volume/non-hydrogen atom is smaller than normal (17.8 Å³ in the pharmaceuticals we have studied), at 16.6 Å³.

The Bravais–Friedel–Donnay–Harker (Bravais, 1866; Friedel, 1907; Donnay and Harker, 1937) morphology suggests that we might expect platy morphology for molnupiravir, with {001} as the major faces. A second-order spherical harmonic model was included in the refinement. The texture index was 1.001, indicating an insignificant preferred orientation in this rotated capillary specimen.

IV. DEPOSITED DATA

The powder pattern of molnupiravir Form I from this synchrotron data set has been submitted to ICDD for the Powder Diffraction File. CIF files from the Rietveld refinement and

DFT geometry optimization were also deposited and can be requested at pdj@icdd.com.

ACKNOWLEDGMENTS

Use of the Advanced Photon Source at Argonne National Laboratory was supported by the U.S. Department of Energy, Office of Science, Office of Basic Energy Sciences, under Contract No. DE-AC02-06CH11357. This work was partially supported by the International Centre for Diffraction Data. We thank Saul Lapidus for his assistance in the data collection.

CONFLICTS OF INTEREST

The authors have no conflicts of interest to declare.

REFERENCES

- Antao, S. M., I. Hassan, J. Wang, P. L. Lee, and B. H. Toby. 2008. "State-of-the-Art High-Resolution Powder X-Ray Diffraction (HRPXRD) Illustrated with Rietveld Refinement of Quartz, Sodalite, Tremolite, and Meionite." *Canadian Mineralogist* 46: 1501–09.
- Bade, R., J. R. Bothe, E. Sirota, A. P. J. Brunskill, J. A. Newman, Y. Zhang, M. Tan, M. Zheng, G. Brito, M. Poirer, P. S. Fier, Y. Xu, M. D. Ward, K. Stone, I. H. Lee, A. J. Gitter, F. Bernardoni, M. A. Zompa, H. Luo, S. Patel, T. Masiuk, J. Mora, T. Ni, G. A. Koh, J. Tarabakija, J. Liu, M. B. Lowinger, and T. Mahmood. 2023. "Polymorphs, Particle Size, and a Pandemic: Development of a Scalable Crystallization Process for Molnupiravir, an Antiviral for the Treatment of COVID-19." *Organic Process Research & Development* 27: 2100.
- Bothe, J. R., A. P. J. Brunskill, M. Lockwood, J. A. Newman, and M. T. Saindane. 2022. "Novel Forms of Antiviral Nucleosides." International Patent Application WO 2022/047229 A1.
- Bravais, A. 1866. *Etudes Cristallographiques*. Gauthier Villars.
- Bruno, I. J., J. C. Cole, M. Kessler, J. Luo, W. D. S. Motherwell, L. H. Purkis, B. R. Smith, R. Taylor, R. I. Cooper, S. E. Harris, and A. G. Orpen. 2004. "Retrieval of Crystallographically-Derived Molecular Geometry Information." *Journal of Chemical Information and Computer Sciences* 44: 2133–44.
- Caraco, Y., G. E. Crofoot, P. A. Moncada, A. N. Galustyan, D. B. Musungaie, B. Payne, E. Kovalchuk, A. Gonzalez, M. L. Brown, A. Williams-Diaz, W. Gao, J. M. Strizki, J. Grobler, J. Du, C. A. Assaid, A. Paschke, J. R. Butters, M. G. Johnson, and C. De Anda; for the MOVE-OUT Study Group. 2022. "Phase 2/3 Trial of Molnupiravir for Treatment of COVID-19 in Nonhospitalized Adults." *NEJM Evidence* 1: 25. doi:10.1056/evidoa2100043.
- Cavazzoni, P. A. 2023. "Molnupiravir Emergency Use Authorization 108." www.fda.gov/media/155053/download.
- Dassault Systèmes. 2023. *BIOVIA Materials Studio 2024*. BIOVIA.
- Donnay, J. D. H., and D. Harker. 1937. "A New Law of Crystal Morphology Extending the Law of Bravais." *American Mineralogist* 22: 446–67.
- Erba, A., J. K. Desmaris, S. Casassa, B. Civalleri, L. Donà, I. J. Bush, B. Searle, L. Maschio, L.-E. Daga, A. Cossard, C. Ribaldone, E. Ascrizzi, N. L. Marana, J.-P. Flament, and B. Kirtman. 2023. "CRYSTAL23: A Program for Computational Solid State Physics and Chemistry." *Journal of Chemical Theory and Computation* 19: 6891–932. doi:10.1021/acs.jctc.2c00958.
- Favre-Nicolin, V., and R. Černý. 2002. "FOX, Free Objects for Crystallography: A Modular Approach to Ab Initio Structure Determination from Powder Diffraction." *Journal of Applied Crystallography* 35: 734–43.
- Friedel, G. 1907. "Etudes sur la loi de Bravais." *Bulletin de la Société Française de Minéralogie* 30: 326–455.
- Gatti, C., V. R. Saunders, and C. Roetti. 1994. "Crystal-Field Effects on the Topological Properties of the Electron-Density in Molecular Crystals: The Case of Urea." *Journal of Chemical Physics* 101: 10686–96.
- Han, P., L. Wang, S. Song, C. Yao, X. Tao, G. Xie, H. Li, Y. Qu, H. Wang, Z. Gao, Y. Sun, H. Wu, and W. Song. 2024. "Polymorphs and Solvates of Molnupiravir: Crystal Structures and Solid Forms Transformation Analysis." *Crystal Growth & Design* 24: 4758–69.
- Hirshfeld, F. L. 1977. "Bonded-Atom Fragments for Describing Molecular Charge Densities." *Theoretica Chimica Acta* 44: 129–38.
- Imran, M., M. K. Arora, S. M. B. Asdaq, S. A. Khan, S. I. Alaql, M. K. Alshammari, M. M. Alshehri, A. S. Alshrari, A. M. Ali, A. M. Al-shammeri, B. D. Alhazmi, A. A. Harshan, M. T. Alam, and Abida. 2021. "Discovery, Development, and Patent Trends on Molnupiravir; A Projective Oral Treatment for COVID-19." *Molecules* 26: 5795. doi:10.3390/molecules26195795.
- Kabekkodu, S. N., A. Dosen, and T. N. Blanton. 2024. "PDF-5+ : A Comprehensive Powder Diffraction File™ for Materials Characterization." *Powder Diffraction* 39: 47–59.
- Kaduk, J. A., C. E. Crowder, K. Zhong, T. G. Fawcett, and M. R. Suchomel. 2014. "Crystal Structure of Atomoxetine Hydrochloride (Strattera), C₁₇H₂₂NOCl." *Powder Diffraction* 29: 269–73.
- Kresse, G., and J. Furthmüller. 1996. "Efficiency of Ab-Initio Total Energy Calculations for Metals and Semiconductors Using a Plane-Wave Basis Set." *Computational Materials Science* 6: 15–50.
- Lee, P. L., D. Shu, M. Ramanathan, C. Preissner, J. Wang, M. A. Beno, R. B. Von Dreele, L. Ribaud, C. Kurtz, S. M. Antao, X. Jiao, and B. H. Toby. 2008. "A Twelve-Analyzer Detector System for High-Resolution Powder Diffraction." *Journal of Synchrotron Radiation* 15: 427–32.
- Macrae, C. F., I. Sovago, S. J. Cottrell, P. T. A. Galek, P. McCabe, E. Pidcock, M. Platings, G. P. Shields, J. S. Stevens, M. Towler, and P. A. Wood. 2020. "Mercury 4.0: From Visualization to Design and Prediction." *Journal of Applied Crystallography* 53: 226–35.
- Materials Design. 2023. *Medea 3.7.2*. Materials Design Inc.
- Painter, G. R., M. G. Natchus, O. Cohen, W. Holman, and W. P. Painter. 2021. "Developing a Direct Acting, Orally Available Antiviral Agent in a Pandemic: The Evolution of Molnupiravir as a Potential Treatment for COVID-19." *Current Opinion in Virology* 50: 17–22. doi:10.1016/j.coviro.2021.06.003.
- Rammohan, A., and J. A. Kaduk. 2018. "Crystal Structures of Alkali Metal (Group 1) Citrate Salts." *Acta Crystallographica Section B: Crystal Engineering and Materials* 74: 239–52. doi:10.1107/S2052520618002330.
- Singh, A. K., A. Singh, R. Singh, and A. Misra. 2021. "Molnupiravir in COVID-19: A Systematic Review of Literature." *Diabetes & Metabolic Syndrome* 15: 102329. doi:10.1016/j.dsx.2021.102329.
- Spackman, P. R., M. J. Turner, J. J. McKinnon, S. K. Wolff, D. J. Grimwood, D. Jayatilaka, and M. A. Spackman. 2021. "Crystalexplorer: A Program for Hirshfeld Surface Analysis, Visualization and Quantitative Analysis of Molecular Crystals." *Journal of Applied* 54: 1006–11.
- Sykes, R. A., P. McCabe, F. H. Allen, G. M. Battle, I. J. Bruno, and P. A. Wood. 2011. "New Software for Statistical Analysis of Cambridge Structural Database Data." *Journal of Applied Crystallography* 44: 882–86.
- Toby, B. H., and R. B. Von Dreele. 2013. "GSAS II: The Genesis of a Modern Open Source All Purpose Crystallography Software Package." *Journal of Applied Crystallography* 46: 544–49.
- van de Streek, J., and M. A. Neumann. 2014. "Validation of Molecular Crystal Structures from Powder Diffraction Data with Dispersion-Corrected Density Functional Theory (DFT-D)." *Acta Crystallographica Section B: Structural Science, Crystal Engineering and Materials* 70: 1020–32.
- Wang, J., B. H. Toby, P. L. Lee, L. Ribaud, S. M. Antao, C. Kurtz, M. Ramanathan, R. B. Von Dreele, and M. A. Beno. 2008. "A Dedicated Powder Diffraction Beamline at the Advanced Photon Source: Commissioning and Early Operational Results." *Review of Scientific Instruments* 79: 085105.
- Wavefunction, Inc. 2023. *Spartan '24. V. 1.0.0*. Wavefunction Inc.
- Xuchun, Z., Z. Yiping, and F. Chenchen. 2021. "Molnupiravir Crystal Form A and Preparation Method Thereof." Chinese Patent CN112778387 A.